

Limitation in velocity of converging shock wave

S. G. Chefranov, Ya. E. Krasik and A. Rososhek

Physics Department, Technion, Haifa 32000, Israel

The commonly applied self-similar solution of the problem of the converging shock wave (shock) evolution with constant compression of the medium behind the shock front results in the unlimited increase of the medium velocity in the vicinity of the implosion. In this paper, the convergence of cylindrical shocks in water is analyzed using the mass conservation law, when the water compression behind the shock front is a variable. The model predicts a finite range of radii, which depends on the adiabatic index of water and where the increase in pressure exceeds the sum of the change of the kinetic and internal energy densities behind the shock front. In this range of radii only finite increase of the shock and water flow velocities is realized.

I. Introduction

Research studies of the evolution of converging spherical and cylindrical shocks are important for fundamental and applied problems related to the behavior of matter under extreme conditions, controlled thermonuclear fusion, and astrophysics.^{1,2} In this research, the self-similar shock implosion approach is frequently used.³ This approach considers an adiabatic ideal gas with a polytropic index $n > 1$ and maximal constant compression $\delta = (\rho_1/\rho_0) = (n + 1)/(n - 1)$ behind the shock front. Here ρ_1 and ρ_0 are the densities of the gas behind the shock front and at normal conditions, respectively. This approach does not consider the radiation losses of the compressed medium and the shock instabilities or the dynamics of the piston that generates this shock. This model yields an unlimited shock velocity and, consequently, pressure in the vicinity of the implosion. For example, in Ref. 4, using the self-similar approach for converging spherical and cylindrical shock implosions, the dependence $D_2 = D_1(R_2/R_1)^{-(1-\alpha)/\alpha}$ was determined. Here, $R(t) = A(-t)^\alpha$; $D = dR/dt = -\alpha A^{\frac{1}{\alpha}} R^{-\frac{1-\alpha}{\alpha}}$ is the shock radius and its front velocity, $\alpha = 0.6, 0.75$ are the self-similarity parameters for spherical and cylindrical shocks, respectively, and the indexes “1” and “2” correspond to the radii of convergence R_1 and $R_2 < R_1$. Thus, for given values of D_1 at R_1 , the dependence $D_2(R_2)$ is calculated.

The self-similar approach describes the evolution of shock implosion velocity in the range of radii without accounting information associated with the separation of the shock from the piston. However, when the shock has not yet separated from the piston, the shock evolution is determined by the piston velocity.³ The evolution of the shock in the intermediate range of radii, i.e., the range where, despite a continuing increase in the distance between the shock and piston,

the parameters of the shock can be influenced by its parameters shortly after its separation from the piston, remains unclear.

In this study, a description of the converging cylindrical shock evolution in water in this intermediate range of radii is presented. In Section II, using the mass conservation law, Rankine-Hugoniot relations, and the equation of state (EOS) of water, the pressure, water compression, and flow velocity behind the shock front are obtained versus the shock radius. In Section III, the range of radii, where the increase of pressure exceeds the increase in the sum of the kinetic and internal energy densities behind the shock front, is determined.

II. Mass conservation law and quasi-self-similar shock wave convergence

Let us consider the convergence of cylindrical shock in water with a front of R_1 at time t_1 and R_2 at time t_2 (see Fig. 1).

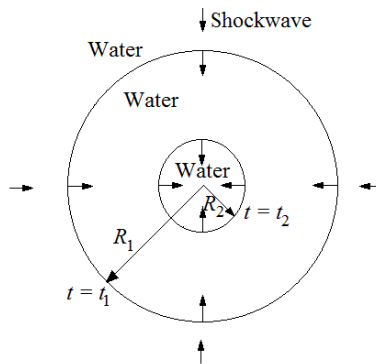


Fig. 1. Converging cylindrical shock in water with shock front at two time instants $t = t_1$ and $t = t_2$ corresponding to radii R_1 and R_2 , respectively.

The densities of water behind the shock front at t_1 and t_2 are ρ_1 and ρ_2 , respectively. Let us introduce the dimensionless parameters: $\delta_1 = \rho_1/\rho_0$; $\delta_2 = \rho_2/\rho_0$; $x = R_1/R_2$ and $y = \delta_2/\delta_1 = \rho_2/\rho_1$, where ρ_0 is the density of undisturbed water. The mass conservation law at the shock front³ dictates that $U_a = D_a(\delta_a - 1)/\delta_a$, where D_a is the shock velocity and U_a is the velocity

of the water flow behind the shock front. The index $a = 1, 2$ is related to time t_1 or t_2 . Let us consider the continuity equation for the cylindrical case with azimuthal symmetry:

$$\frac{\partial \rho}{\partial t} + \frac{1}{r} \frac{\partial}{\partial r} r \rho U = 0 \quad (1)$$

In the laboratory coordinate system, we consider a water layer bounded by radii R_1 and R_2 (see Fig. 1). The shock propagates with velocities $D_1 = -|D_1|$ and $D_2 = -|D_2|$ at times t_1 and t_2 , respectively. Let us integrate (1) over the layer bounded by radii R_2 and R_1 :

$$\frac{\partial}{\partial t} \int_{R_2}^{R_1} dr r \rho(r, t) + R_1 \rho(R_1, t) U(R_1, t) - R_2 \rho(R_2, t) U(R_2, t) = 0 \quad (2)$$

In Refs. 5 and 6, the collapse of a vacuum cavity in an incompressible medium when $\rho = \rho_0 = \text{const}$ was analyzed using a self-similar power law $U(r, t)r = q(t) = U(R_c(t))R_c(t)$ for the medium velocity $U(r, t)$ versus a radius r and the cavity radius $R_c = R_c(t)$. Here $q(t)$ is only time dependent value. In the case of incompressible medium also from (2) one obtains relation $U(R_2; t) = U(R_1; t)(R_1/R_2)$. This dependence, showed an unlimited increase in the velocity of the medium versus $x = R_1/R_2 \gg 1$. It was noted in Ref. 5 that the compressibility of a liquid should limit the cumulation effect. The effects of compressibility were considered in Refs. 3, 7, and 8, but the obtained self-similar limiting regimes do not allow one to find the limitation in the cumulation due to this effect. The energy dissipation by the shock considered in Ref. 6 for sufficiently large Reynolds numbers, does not prevent unrestricted cumulation when a cavity collapses in an incompressible liquid. In our model, as it will be shown later, the influence of water compressibility on the unlimited increase in the flow velocity near the implosion axis, also does not lead to its finite value. Nevertheless, it will be shown that in the vicinity of

implosion axis, beginning some threshold radius, the increase in the pressure becomes smaller than the sum of kinetic and internal energy densities behind the shock front. The corresponding limit on the shock and water flow velocities is obtained.

Let us consider an analogue of the self-similar power-law^{5,6} for a compressible medium. In this approach, based on the mass conservation law (2), it is possible to obtain the power-law dependence of the medium velocity versus $x = R_1/R_2$. Integration of (2) over time $t = t_1, t \rightarrow \infty$, considering that the first term in (2) has vanished, since at t_1 and $t \rightarrow \infty$ the water density is $\rho = \rho_0$, gives analogue of the quasi-self-similarity case considered in Refs. 5 and 6, but for a compressible medium:

$$\begin{aligned} R_1 I_1 &= R_2 I_2; \\ I_1 &= \int_{t_1}^{\infty} dt \rho(R_1; t) U(R_1; t); \\ I_2 &= \int_{t_2}^{\infty} dt \rho(R_2; t) U(R_2; t) \end{aligned} \quad (3)$$

Here, it was accounted that the medium velocity $U(R_2; t)$ at $r = R_2$ is zero at $t \leq t_2$. Let us consider the mass fluxes balance without contribution of the mass fluxes reflected from the axis. In order to estimate the values of integrals I_1 and I_2 , we assume that the water velocity and density time-dependence can be represented as

$$|U(R_a, t)| = U_a \exp(-\gamma_a(t - t_a)) H(t - t_a); \quad (3.1)$$

$$H(t - t_a) = \begin{cases} 1, & t \geq t_a \\ 0, & t < t_a \end{cases} .$$

$$\rho(R_a; t) = \rho_0 + (\rho_a - \rho_0) \exp(-\gamma_{\rho a}(t - t_a)); a = 1, 2 . \quad (3.2)$$

Here $H(t - t_a)$ is the Heaviside unit step function. In this case, one obtains:

$$I_a = U_a \rho_a f_a; \quad f_a = \frac{1}{\delta_a} \left[\frac{1}{\gamma_a} + \frac{(\delta_a - 1)}{\gamma_a + \gamma_{\rho a}} \right] \quad (3)$$

Let us note that in the case $\gamma_a \gg \gamma_{\rho a}$, $f_a = \gamma_a^{-1}$, when the integrals $I_a = U_a \rho_a \gamma_a^{-1}$. In Fig. 2 one see temporal evolution of the density and flow velocity of water at different radii of cylindrical converging shock generated by underwater electrical explosion of wire array having initial diameter of 10 mm and 4 kJ energy deposited energy into the array within $\sim 1.2 \mu\text{s}$. These dependencies were obtained using one dimensional hydrodynamic simulations⁹ coupled with SESAME EOS for water.¹⁰ Using exponential fit (3.1) and (3.2) (see Fig. 2) for these dependencies, one obtains values of $\gamma_1 \leq 1.52 \mu\text{s}^{-1}$ and $\gamma_{\rho 1} \leq 0.14 \mu\text{s}^{-1}$ for the flow velocity and density, respectively, at radius $R_l = 4 \text{ mm}$. Thus, the approximation $\gamma_1 \gg \gamma_{\rho 1}$ can be considered as reasonable. The same concern is related to smaller converging radii, when also $\gamma_2 \gg |\gamma_{\rho 2}|$. In the general case, the ratio γ_2/γ_1 depends on the radii ratio x . Thus, one obtains from (3) that the flow velocities ratio U_2/U_1 behind the shock front is:

$$\frac{U_2}{U_1} = \frac{x}{y(x)} F; \quad F = \frac{\gamma_2(x)}{\gamma_1} \quad (4)$$

Using exponential fit for the data shown in Fig. 2, one obtains for flow velocity $\gamma_2(x = 10) \approx 5.77 \mu\text{s}^{-1}$. Thus, it is possible to introduce an empirical relation $F(x) \cong x^\beta$; $\beta = \frac{\ln(\gamma_2(x)/\gamma_1)}{\ln x} \approx 0.58$ for $x = 10$. The selection $x = 10$ is based on the estimate (see Section III) where we showed that energetically optimal compression when one obtains excess of the potential energy above the sum of the kinetic and internal energies behind the shock front is limited by the value of the radius $R_2 > R_1/10$, that is $x < 10$.

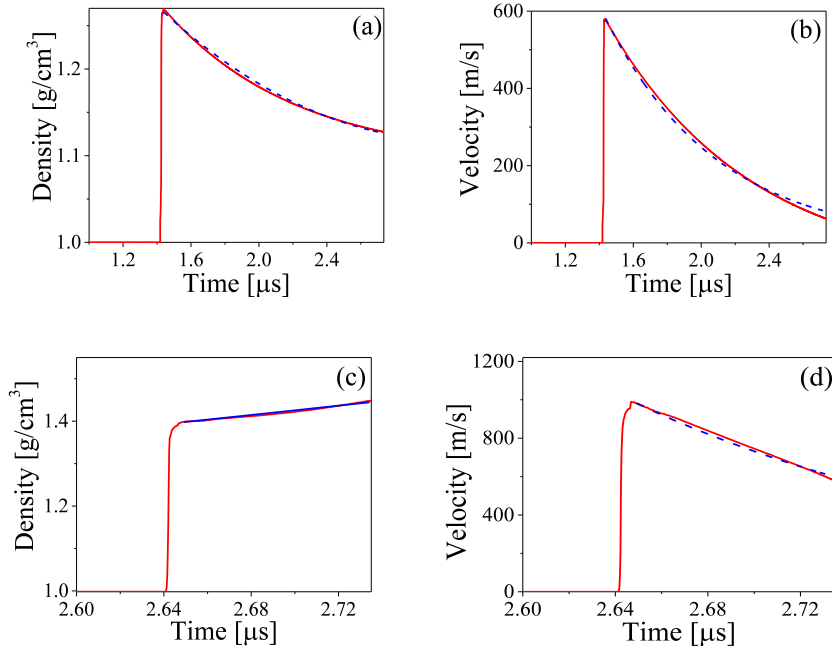


Fig. 2. Density and water flow velocity temporal evolution at the radius of 4 mm (a, b) and radius of 0.4 mm (c, d). Blue (dashed) lines are exponential fit using functions (3.1) and (3.2), where $t_1 = 1.437 \mu\text{s}$ and $t_2 = 2.649 \mu\text{s}$. Red (solid) lines are the results of 1D numerical hydrodynamic simulations coupled with Sesame EOS of water.

To determine the form of function $y(x)$ in (4), let consider this relation together with the Rankine-Hugoniot conditions and the adiabatic EOS of water. From (4) and the Rankine-Hugoniot condition, the shock velocities ratio reads:

$$\frac{D_2}{D_1} = x \frac{(\delta_1 - 1)F}{(y\delta_1 - 1)} \quad (5)$$

Applying the Rankine-Hugoniot condition, the ratio of pressures behind the shock front at radii R_1 and R_2 can be derived from (5) as:

$$\frac{p_2}{p_1} = x \frac{(\delta_1 - 1)F^2}{y(y\delta_1 - 1)} \quad (6)$$

On the other hand, using the isentropic Tait's EOS for water (in the F. D. Murnaghan form),¹¹ $p_a - p_0 = (K_0/n)(\delta_a^n - 1)$, where $K_0 = 22$ kBar; $p_0 \approx 1$ Bar and $n \approx 7.15$, the ratio of pressures for $p > K_0/n \gg p_0$ and $\delta_a^n \gg 1$ is given as:

$$p_2/p_1 = y^n(x) \quad (7)$$

Now, using (6) and (7) one obtains $y(x)$:

$$y^{n+1}(y\delta_1 - 1) = x(\delta_1 - 1)F^2 \quad (8)$$

The dependence of the shock parameters on its radius is determined by relations (4) – (8).

Let us consider approximation $1 \gg 1/\delta_2(n + 2)$, which is always satisfied because $y > 1; n = 7.15$. Thus, the solution of (8) can be presented as:

$$y(x) = \left(\frac{x F^2(x)}{d} \right)^{\frac{1}{n+2}} \frac{1}{\left(1 - \frac{1}{y\delta_1} \right)^{\frac{1}{n+2}}} \approx \left(\frac{x F^2(x)}{d} \right)^{\frac{1}{n+2}} \left(1 + O\left(\frac{1}{(n+2)\delta_2} \right) \right)$$

$$d = \frac{\delta_1}{(\delta_1 - 1)}; F(x) = \frac{\gamma_2(x)}{\gamma_1} = x^\beta; \beta \approx 0.585$$

$$\frac{p_2}{p_1} \approx y^n \approx \left(\frac{x F^2(x)}{d} \right)^{\frac{n}{n+2}}; \quad \frac{u_2}{u_1} \approx (x F(x))^{\frac{n}{n+2}} \left(\frac{\delta_1}{\delta_1 - 1} \right)^{\frac{1}{n+2}} \quad (9)$$

Here let us note that because $y(x) > 1$, the solution for $y(x)$ is valid only for $x > x_{min} = d^{\frac{1}{2(1+\beta)}}$.

For example, for $\beta = 0.58; \delta_1 = 1.25$, one obtains the solution (9) applicability for $x > x_{min} = 1.66$. Let us define the shock convergence described by relations (9) as a quasi-self-similar approach. To avoid confusion with the common self-similarity parameter for cylindrical shock $\alpha \approx 0.75$, we denote this parameter by α_q . The value of the power in (9) can be represented

as $\frac{1}{\alpha_q} - 1$ resulting in

$$\alpha_q = \left(1 + \frac{(1 + \beta)n}{n + 2}\right)^{-1} \quad (10)$$

Thus, for converging cylindrical shock in water one obtains $\alpha_q \approx 0.4$ for $\beta = 0.58$, which is smaller than in the case of the self-similarity approach.

In order to compare (9) with the dependence for the water flow velocity obtained in the model for incompressible water,⁶ we will use similar as in our model, relaxation of velocities at R_1 and R_2 , namely $U(R_1; t) = U_1 \exp(-\gamma_1 t)$; $U(R_2; t) = U_2 \exp(-\gamma_2 t)$; $\gamma_2 = \gamma_2(x)$. After integration over time from zero to infinity, one obtains:

$$U_2 = U_1 \frac{\gamma_2 R_1}{\gamma_1 R_2} = U_1 \left(\frac{R_1}{R_2}\right)^{1+\beta} ; \frac{\gamma_2}{\gamma_1} = \left(\frac{R_1}{R_2}\right)^\beta ; \beta = \ln\left(\frac{\gamma_2}{\gamma_1}\right) \ln^{-1}\left(\frac{R_1}{R_2}\right)$$

Let us assume that in an incompressible medium, the indices of the velocity relaxation is close to $\beta = 0.58$ (see Fig. 2). In this case, one obtains a power-law dependence $U_2 = U_1 \left(\frac{R_1}{R_2}\right)^{1.58}$, which is shown in Fig. 3 together with the radial dependence of the velocity in the case of compressible water. In the latter case, using (9) and $n = 7.15$; $\beta = 0.58$, the mass conservation law leads to the radial dependence for the flow velocity:

$$U_2 = U_1 \left(\frac{\rho_1}{\rho_1 - \rho_0}\right)^{\frac{1}{9.15}} \left(\frac{R_1}{R_2}\right)^{1.24}$$

One can see that the compressibility leads to a slower increase in the velocity of water which is related to the additional energy losses for water compression. However, water compressibility does not eliminate an unlimited increase in the flow velocity.

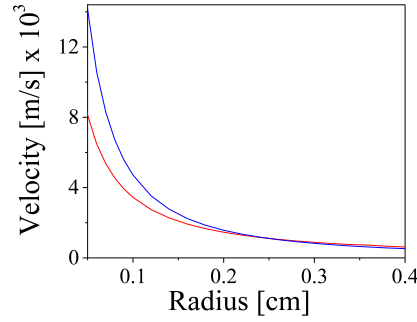


Fig. 3. Dependencies of the of flow velocity vs. radius for compressible (red) and incompressible (blue)^{5,6} water.

The value of power, 1.24, in (9) is significantly (~ 3.76) larger than the value of power, (0.33) in common self-similar solution,³ which considers constant entropy of ideal gas compressed to its maximal value behind the shock front. Here let us note that the geometric factor, which is necessary to account to satisfy the integral law of conservation of mass (2) and (3), leads to the value of exponent power larger than 1, as in a cylindrical case of an incompressible water considered in Ref. 6. Thus, additional studies related to how the self-similar solution³ satisfies the integral form of the mass conservation law, are required.

The quasi-self-similar solution (9) does not considered energy dissipation processes behind the shock front, which are realized in experiments and are accounted in hydrodynamic simulations coupled with EOS for water.⁹ To account the energy dissipation in our model, we will use the results of numerical simulations of the water flow velocity relaxation (see Fig. 2). In this case, the flow velocities ratio instead of (9) can be presented as:

$$\frac{\bar{u}_2}{\bar{u}_1} = \frac{u_2}{u_1} \exp(-\gamma_1 x^\mu (t_2(x) - t_1)) \quad (11)$$

Here, differing to relation (3.1), where the flow velocity temporal relaxation is related to a fixed radius, the ratio (11) determines the process of the energy dissipation during the shock

propagation from a larger to smaller radii. Here we assume that an exponential factor in (11), responsible for energy dissipation, does not prevent the use of the isothermal EOS for water and the Rankine-Hugoniot relations for ratio U_2/U_1 determined by (9). In Fig. 4(a), the dependence \tilde{U}_2/\tilde{U}_1 [see (11)] versus ratio of radii x is shown. Here values of $\mu(x)$ [see Fig. 4(b)] were determined using the fit of \tilde{U}_2/\tilde{U}_1 with the results of one dimensional hydrodynamic numerical simulations of the shock convergence for the same conditions as in Fig. 2. In the Fig. 4(a) we also show the dependence of $\frac{U_2}{U_1} = f(x)$ which follows from (9). One can see that quasi-self-similar solution (9) as expected, differs strongly from numerical simulations and shows necessity for energy dissipation accounting.

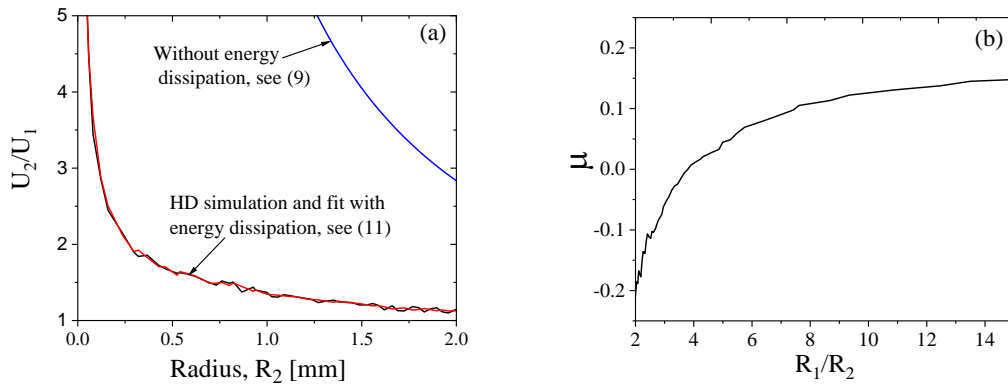


Fig. 4. Water flow velocities ratio vs. the radius of convergence (a) and values of μ vs. radii ratio (b).

In the case $x \gg 1$, the value $t_2(x) - t_1 \rightarrow t_F - t_1 = \text{const}$, where t_F is the time when the shock approaches the implosion axis. Thus, in the vicinity of implosion, increase in energy dissipation occurs solely due to the increasing of x^μ in (11), thus limiting the increase in water flow velocity. Indeed, in the limit $x \gg 1$; $t_2 \rightarrow t_F \approx 2.73 \mu\text{s}$ (see Fig. 2) and using (9), the ratio (11) reads:

$$\frac{\tilde{U}_2}{\tilde{U}_1} = Ax^a \exp(-Bx^\mu);$$

$$A \approx 1.19; a = 1.23; B = 2.02; \mu = 0.125 \quad (12)$$

This flow velocities ratio has a maximum at $x_{d_max} = \frac{1}{\mu} \ln\left(\frac{a}{B\mu}\right) \approx 12.7$, which determines maximal radius to which water velocity increases behind the shock front. In Ref. 6, a similar effect of limited energy accumulation was obtained due to the viscosity effects for the Reynolds numbers smaller than a threshold value.

III. Energy-optimal compression range of converging radii

In this section, it will be shown that even without accounting the energy dissipation, there is a restriction on the range of radii $x < x_{max}$ related to a violation of the energetically optimal compression mode. Using relations (4) – (9), one can determine this range of radii, when the increase in the pressure exceeds the increase in the sum of the kinetic and internal energy densities of the water flow. The average kinetic energy density transferred by the shock to the water flow behind its front during $\Delta t = t_2 - t_1$ can be defined as $\Delta E_K = \rho_2 \frac{U_2^2}{2} - \rho_1 \frac{U_1^2}{2}$. Using the Rankine-Hugoniot relations, the change in kinetic energy density reads

$$\Delta E_K = \frac{\rho_1 U_1^2}{2} \left(y \frac{U_2^2}{U_1^2} - 1 \right) \equiv \frac{p_1}{2} \left(\frac{p_2}{p_1} (y\delta_1 - 1) - \delta_1 + 1 \right) \quad (13)$$

The change in the internal energy density $\Delta E_I = E_2 - E_1$, calculated using (4) and (6), when $\rho_1 U_1^2 = p_1(\delta_1 - 1)$ and the Rankine-Hugoniot condition³ $E_a = \varepsilon_a \rho_a$, $\varepsilon_a - \varepsilon_0 = \frac{(p_a + p_0)}{2} \left(\frac{1}{\rho_0} - \frac{1}{\rho_a} \right)$ for $p_a \gg p_0$, $E_a \gg \delta_a E_0$, is found to be equal to ΔE_K . Let us note that the value of ΔE_I was

obtained using only the Rankine-Hugoniot condition. In the general case, the value of ΔE_I , in addition to the thermal component associated to the thermal motion of particles, should also include a change in the potential energy of the interaction of these particles (see Eq. 8.4 in Ref. 13). Here let us note that the equality $\Delta E_I = \Delta E_K$ agrees with the data presented in Ref. 14 regarding shocks in water where also was shown that the condition $\Delta E_P > \Delta E_I + \Delta E_K$ is valid only for pressures below some threshold value.

The change in the pressure during Δt can be written as

$$\Delta E_P = p_1 \left(\frac{p_2}{p_1} - 1 \right) \quad (14)$$

Now, let us estimate the minimal shock radius for which the energy compression ($\Delta E_P > \Delta E_I + \Delta E_K$) is optimal. Below this radius, the increase in the sum of the change in the kinetic and internal energy densities exceeds the increase in the pressure change; i.e., $\Delta E_K + \Delta E_I = 2\Delta E_K > \Delta E_P$. In the latter case, for instance, hydrodynamic instability may occur, leading to the appearance of swirling vortex motion (see Refs. 6, 15 and 16) which can change the water flow's radial convergence. Using (13) and (14), condition $\Delta E_P > 2\Delta E_K$ reads

$$y^n(2 - \delta_1 y) > 2 - \delta_1 \quad (13)$$

One can see that, for $\delta_1 < 2$, the condition $y < y_{max} = 2/\delta_1$ should be satisfied. Thus, for instance for $\delta_1 = 1.25$ inequality (13) is valid for $1 < y < y_t = 1.6$, when $y_t \approx y_{max} = 2/\delta_1$.

Using (9) for y , the range of radii within which $\Delta E_P > 2\Delta E_K$ is valid can be obtained as

$$x < x_{max} = \left(\frac{2^{n+2}}{(\delta_1 - 1)\delta_1^{n+1}} \right)^{\frac{1}{2(1+\beta)}}$$

$$R_2 > R_{2min} = R_1/x_{max} \quad (14)$$

Applying (14), for instance for $\delta_1 = 1.25$, one obtains $R_{2min} \approx 0.15R_1$, which is almost twice the radius $x_{d,max}$ obtained in section II. Thus, when condition (14) is satisfied, an energetically optimal compression can be realized.

Finally, using (9) and (14), one can estimate that, for the quasi-self-similar mode, the maximum pressure when the shock approaches R_{2min} is

$$p_{2max} \approx p_1 \left(\frac{2}{\delta_1} \right)^n = \frac{K_0}{n} (\delta_1^n - 1) \left(\frac{2}{\delta_1} \right)^n \approx 2^n \frac{K_0}{n} \quad (15)$$

For implosion in water, for $n = 7.15$, the maximal pressure is $p_{2max} = 440 \text{ kBar}$. One can see that the maximum pressure value in the vicinity of implosion is independent of the initial compression of the converging shock and its value depends only on the adiabatic index, which in general depends on the pressure.¹¹

IV. Summary

Based on the mass conservation law, the model for converging cylindrical shock waves is suggested. The suggested model considers conservation laws in the form of the Hugoniot relations and the integral form of the mass conservation law. The limits of applicability of these laws relate to dissipation processes which were not accounted in our basic model. In addition, we use the isothermal EOS for water which applicability is limited by pressures of a few hundreds of kBar. However, a more significant limitation actually relates to the value of the index n in the EOS which is considered constant. In general case, the value of n depends on temperature and, respectively, on pressure and density. Nevertheless, this model predicts the finite energy-optimal range of the radii of the converging shocks, in which ultra-high, but however limited pressures can be obtained behind the shock front.

Acknowledgments

We thank A. Velikovich, J. Leopold, V. Gurovich, A. Virozub and S. Bland for fruitful discussions and comments. This research was supported by the Israeli Science Foundation Grant No. 492/18.

References

1. V. E. Fortov and I. T. Iakubov, *The Physics of Non-Ideal Plasma* (World Scientific Publishing Co. Pte. Ltd., Singapore, 2000).
2. R. P. Drake, *High Energy Physics: Fundamentals, Inertial Fusion and Experimental Astrophysics* (Springer, New York, 2006).
3. Ya. B. Zel'dovich and Yu. P. Raizer, *Physics of Shock Waves and High – Temperature Hydrodynamic Phenomena*, 2nd ed. (Academic, New York, 1967).
4. A. Grinenko, V. Tz. Gurovich, and Ya. E. Krasik, *Phys. Plasmas* **14**, 012701 (2007).
5. Lord Rayleigh, *Phil. Mag.* **34**, 94 (1917). <http://dx.doi.org/10.1080/14786440808635681>
6. E. I. Zababahin and I. E. Zababahin, “*The phenomena of unlimited cumulation*”, (in Russian, Moscow, Nauka, 1988).
7. C. Hunter, *J. Fluid Mech.* **8**, 241 (1960).
8. J. F. Giron, S. D. Ramsey, and R.S. Baty, *Phys. Rev. E* **101**, 053101 (2020).
9. G. Bazalitski, V. Ts. Gurovich, A. Fedotov-Gefen, S. Efimov, and Ya. E. Krasik, *Intern. J. Shock Waves, Detonations and Explosions* **21**, 321 (2011).
10. SESAME: The Los Alamos National Laboratory Equation-of-State Database, edited by S. P. Lyon and J. D. Johnson, Los Alamos National Laboratory, Report No. LA-UR-92-3407, 1992.
11. S. Ridah, Shock waves in water, *J. Appl. Phys.*, **64**, 152 (1988); <https://doi.org/10.1063/1.341448>

12. R. B. Lazarus, SIAM J. Numer. Anal. **18**, 316 (1981).
13. L. D. Landau and E. M. Lifshitz, *Theoretical Physics, Mechanics*, (Moscow, 2004).
14. M. H. Rice, and J. M. Walsh, Equation of state of water to 250 Kilobars, J. Chem. Phys., **26**, 824 (1957); <https://doi.org/10.1063/1.1743415>
15. A. S. Chefranov, and S. G. Chefranov, Extrema of the kinetic energy and its dissipation rate in vortex flows, Doklady Physics, **48** (12), 696 (2003)
16. S. G. Chefranov, Instability of cumulation in convergent cylindrical shock wave, Phys. Fluids, **33**, 096111 (2021); <https://doi.org/10.1063/5.0065017>